Mon. Not. R. Astron. Soc. **341,** L1–L6 (2003)

The radio–mid-infrared correlation and the contribution of 15-μm galaxies to the 1.4-GHz source counts

C. Gruppioni,[1,2]★ F. Pozzi,[2,3] G. Zamorani,[2,4] P. Ciliegi,[2] C. Lari,[4]
E. Calabrese,[2] F. La Franca[5] and I. Matute[5]

[1]*Istituto Nazionale di Astrofisica: Osservatorio Astronomico di Padova, vicolo dell'Osservatorio 5, I-35122 Padova, Italy*
[2]*Istituto Nazionale di Astrofisica: Osservatorio Astronomico di Bologna, via Ranzani 1, I-40127 Bologna, Italy*
[3]*Dipartimento di Astronomia, Università di Bologna, via Ranzani 1, I-40127 Bologna, Italy*
[4]*Istituto di Radioastronomia del CNR, via Gobetti 101, I-40129 Bologna, Italy*
[5]*Dipartimento di Fisica, Università 'Roma Tre', via della Vasca Navale 84, I-00146 Roma, Italy*

Accepted 2003 March 4. Received 2003 February 18; in original form 2002 October 28

ABSTRACT

The radio counterparts to the 15-μm sources in the European Large Area *ISO* Survey southern fields are identified in 1.4-GHz maps down to ∼80 μJy. The radio–mid-infrared correlation is investigated and derived for the first time at these flux densities for a sample of this size. Our results show that radio and mid-infrared (MIR) luminosities correlate almost as well as radio and far-infrared (FIR), at least up to $z \simeq 0.6$. Using the derived relation and its spread together with the observed 15-μm counts, we have estimated the expected contribution of the 15-μm extragalactic populations to the radio source counts and the role of MIR starburst galaxies in the well-known 1.4-GHz source excess observed at sub-mJy levels. Our analysis demonstrates that IR emitting starburst galaxies do not contribute significantly to the 1.4-GHz counts for strong sources, but start to become a significant fraction of the radio source population at flux densities $\lesssim$0.5–0.8 mJy. They are expected to be responsible for more than 60 per cent of the observed radio counts at $\lesssim$0.05 mJy. These results are in agreement with the existing results on optical identifications of faint radio sources.

Key words: galaxies: evolution – galaxies: starburst – cosmology: observations – infrared: galaxies – radio continuum: galaxies.

1 INTRODUCTION

With a thousand times better sensitivity than the *IRAS* 12-μm data, the LW3 observations (in the 12–18 μm waveband, centred at λ = 15 μm) with the *ISOCAM* camera (Cesarsky et al. 1996) on the *Infrared Space Observatory* (*ISO*; Kessler et al. 1996) have allowed us for the first time to perform sensitive surveys of distant infrared galaxies (up to $z \sim 1.5$) in the mid-infrared (MIR) band. The extragalactic source counts derived from these 15-μm surveys, including large area shallow surveys like ELAIS (Oliver et al. 2000) covering the flux density range $0.5 \leqslant S_{15\,\mu m} \leqslant 150$ mJy (Lari et al. 2001), and small area deep integrations reaching $S_{15\,\mu m} \simeq 0.05$–0.1 mJy (Elbaz et al. 1999), show a strong departure from no evolution predictions at low flux densities ($\leqslant$1–2 mJy; Elbaz et al. 1999; Gruppioni et al. 2002). According to both optical identification works (Aussel et al. 1999; Elbaz et al. 1999; Pozzi et al. 2003) and theoretical models (i.e. Franceschini et al. 2001), the sources responsible for the sharp upturn observed in the number counts at faint flux densities are mainly star-forming galaxies at moderately high redshifts ($0.4 \leqslant z \leqslant 1.4$).

A tight correlation between far-infrared (FIR) and radio continuum for star-forming galaxies is locally well assessed over a large range of luminosities, from normal spirals to the more extreme ultraluminous infrared galaxies (ULIGS: $L > 10^{12}$ L$_{\odot}$), as shown by several authors (Condon 1992; Cram et al. 1998; Yun, Reddy & Condon 2001). So far there have been many attempts to explain the tightness of this correlation, whose origin is still somewhat unclear. It is generally assumed that massive stars are responsible for both the ultraviolet (UV) photons heating the dust, which re-radiates in the infrared band, and the acceleration of relativistic electrons, producing the radio continuum, after their explosion as supernovae. Such a tight local correlation does not necessarily hold in the distant Universe and, even in this case, it would be interesting to investigate possible variations with redshift of the slope and/or normalization of the correlation. Moreover, it is not obvious that the radio continuum should correlate with the MIR emission (produced by a mixture of stochastic heating from polycyclic aromatic hydrocarbons (PAHs;

★E-mail: gruppioni@bo.astro.it

i.e. Puget & Léger 1989) and thermal emission at high temperature) as well as with the FIR (resulting from thermal emission of large dust grains at lower temperature).

The aim of this paper is to study for the first time the radio–MIR correlation for galaxies at cosmological redshifts through a statistically significant sample. The considered sample contains 65 sources detected at both 15 μm and 1.4 GHz in the ELAIS southern fields, all identified with galaxies up to $z \sim 0.8$. By introducing the radio–MIR correlation into the evolutionary model that fits the 15-μm extragalactic source counts (see Gruppioni et al. 2002), we have then estimated the expected contribution to the radio source counts from the MIR star-forming galaxies, whose role and importance relative to that of active galactic nuclei (AGN) in the 1.4-GHz excess of sub-mJy/μJy radio sources is still matter of debate.

The paper is structured as follows. In Section 2 we present our data sample. In Section 3 we derive the radio–MIR correlation and investigate its redshift dependence. In Section 4 we estimate the contribution of infrared star-forming galaxies to the radio source counts and discuss the results and implications. In Section 5 we present our conclusions.

Throughout this paper we will assume $H_0 = 75$ km s^{-1} Mpc^{-1}, $\Omega_m = 0.3$ and $\Omega_\Lambda = 0.7$.

2 THE DATA SAMPLES

The ELAIS survey at 15 μm (Oliver et al. 2000), performed in raster mode with the *ISOCAM* instrument, covers a total area of ∼12 deg^2 divided into four main fields and several smaller areas. One of the main fields, S1, and one of the smaller areas, S2, are located in the southern hemisphere. S1 is centred at $\alpha(2000) = 00^{\rm h}34^{\rm m}44\overset{\rm s}{.}4$, $\delta(2000) = -43°28'12''$ and covers an area of 2° × 2°, while S2 is centred at $\alpha(2000) = 05^{\rm h}02^{\rm m}24\overset{\rm s}{.}5$, $\delta(2000) = -30°36'00''$ and covers an area of 21 × 21 arcmin. The 15-μm data in these fields have been reduced and analysed using the LARI technique, especially developed for the detection of faint sources (Lari et al. 2001), obtaining two samples at $\geqslant 5\sigma$ that contain 462 sources with $0.5 \lesssim S_{15\,\mu\rm m} \lesssim 150$ mJy in S1 (available at http://www.bo.astro.it/∼elais/catalogues/ELAIS_CAM_15micron_S1.TAB) and 43 sources with $S_{15\,\mu\rm m} \gtrsim 0.4$ mJy in the deeper field S2, respectively. The 15-μm source counts have been derived by Gruppioni et al. (2002) using the ∼320 extragalactic sources detected over the S1 area.

The whole S1 and S2 areas have been surveyed in the radio with the Australia Telescope Compact Array to $S_{1.4\,\rm GHz} \simeq 0.2$ and 0.13 mJy, respectively (Gruppioni, Mignoli & Zamorani 1999; Ciliegi et al., in preparation) and in several optical bands: S1 in the *R* band (to $R \sim 22.5$) with the ESO/Danish 1.5-m Telescope, and S2 in the *U*, *B*, *R* and *I* bands with the WFI at the ESO 2.2-m Telescope and in the K' band with SOFI at the ESO NTT. The radio catalogue in S1 (available at http://www.bo.astro.it/∼elais/catalogues/ELAIS_RADIO_S1.TAB) consists of 652 1.4-GHz sources detected at the 5σ level, while the S2 radio catalogue consists of 75 sources.

Spectroscopic observations of the optical counterparts of the *ISOCAM* sources were carried out at the 2dF/AAT and ESO Danish 1.5-m, 3.6-m and NTT telescopes. In S1 all the sources with $R < 21.0$ have been spectroscopically identified (∼210 extragalactic objects; La Franca et al., in preparation). In S2 we have spectroscopic information for 29 sources brighter than $R \simeq 21$ (about 68 per cent of the sample; Pozzi et al. 2003) obtained with the ESO 3.6-m telescope.

3 THE RADIO-MIR CORRELATION

In order to investigate the radio–MIR correlation within our *ISOCAM* sample, we have first cross-correlated the 15-μm and the 1.4-GHz catalogues (complete at the 5σ level) in S1 and S2, finding 28 and 13 coincidences, respectively, within a distance of 5 arcsec. Note that the S1 15-μm catalogue considered for this analysis is the same, conservative, catalogue used to derive the source counts (see Gruppioni et al. 2002), where 35 possibly spurious sources (all with $S < 1.5$ mJy) have been excluded after a visual inspection of their pixel history. These sources, detected above the 5σ threshold on the maps obtained through a combination of several images, are too faint to be distinguished from noise on the single pixel histories without uncertainty (see Gruppioni et al. 2002, for further explanation). Then, at each *ISOCAM* position, we have searched for detection in the radio maps down to 3σ, finding 53 additional radio identifications within 5 arcsec (46 in S1 and 7 in S2), for a total of 94 *ISO*–radio associations with $S_{1.4}$ GHz $\geqslant 3\sigma$. The number of expected spurious coincidences, on the basis of the density of *ISO* and radio sources and of the adopted maximum distance (5 arcsec) is of the order of one. 73 of these sources have spectroscopic data and redshift measurements in the spectroscopic data sample available by 2002 October (additional spectra taken in the October run were not used in this work).

In Table 1 we present the percentage of radio detections as a function of the 15-μm flux density. The first two columns give the flux density range and the corresponding average flux density respectively, whilst the following columns give the total number of *ISOCAM* extragalactic objects, the number of radio detections, the number of non-AGN radio detections (in brackets) and the corresponding fraction (i.e. radio detections over total number of extragalactic sources in that bin). At high flux densities all the 15-μm extragalactic sources have a radio counterpart, while the fraction of radio identifications decreases at lower 15-μm flux densities. This is due to the fact that our radio maps are not deep enough to allow the detection of all our 15-μm sources, especially the fainter ones. Fig. 1 (left-hand panel) shows the 1.4-GHz luminosity versus the 15-μm luminosity for the 65 *ISOCAM* galaxies with spectroscopic identification detected in the radio band (open circles). As radio *K*-correction we have applied a power law with a slope $\alpha = 0.7$, whilst at 15 μm we have applied the *K*-corrections derived by Franceschini et al. (2001) using different template spectral energy distributions (SEDs) for the different populations (M82 for starbursts and type 2 AGN, M51 for normal spirals) modelling the 15-μm source counts.

A formal fit to the observed radio–MIR luminosity correlation for the radio detected galaxies only (dashed line) yields

$$\log(L_{1.4\,\rm GHz}/{\rm L}_\odot) = (1.09 \pm 0.05)\log(L_{15\,\mu\rm m}/{\rm L}_\odot) - (5.91 \pm 0.54) \quad (1)$$

Table 1. 15-μm sources detected at 1.4 GHz.

S (mJy)	$\langle S \rangle$	N	$N_{\rm det}$	per cent
<0.5	–	10	0 (0)	0.0
0.5–0.9	0.7	78	11 (11)	14.1
0.9–1.6	1.2	120	19 (17)	15.8
1.6–2.9	2.2	87	28 (27)	32.2
2.9–5.3	3.9	33	14 (11)	42.4
5.3–9.5	7.0	15	12 (11)	80.0
9.5–17.0	12.7	7	6 (5)	85.7
17.0–30.6	22.8	2	2 (1)	100.0
30.6–55.1	41.1	2	2 (1)	100.0

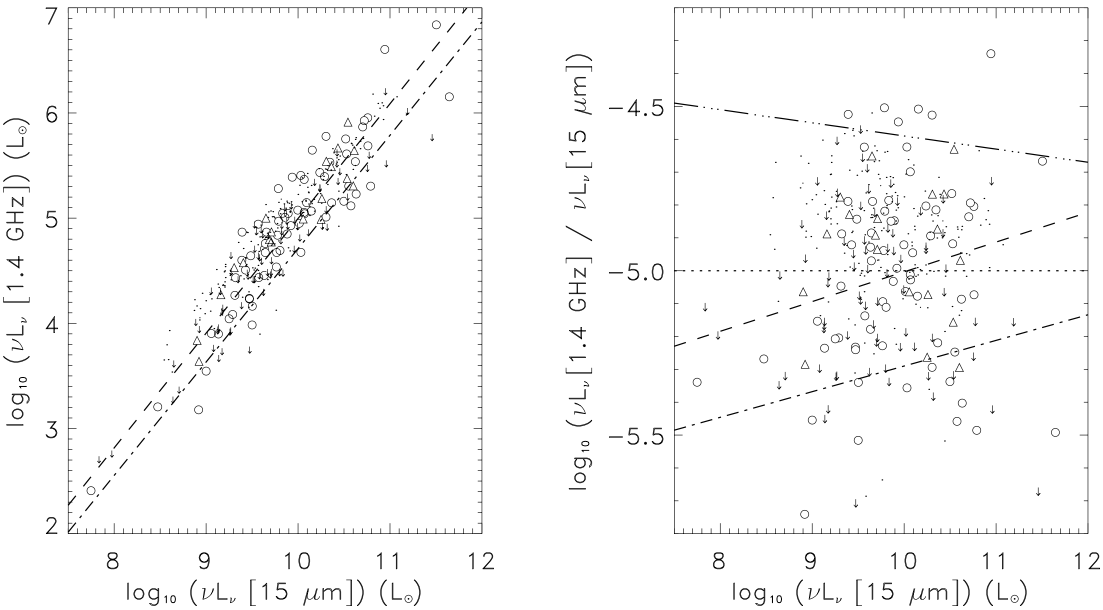

Figure 1. Left-hand panel – radio (1.4 GHz) versus MIR (15 μm) luminosity for the 15-μm galaxies in the ELAIS southern fields. Objects detected in the radio are represented by empty circles (galaxies with spectroscopic redshift) and triangles (without spectroscopic information, to which a redshift has been assigned on the basis of an empirical relation between MIR flux density and z: see text). Arrows are the 3σ radio upper limits with measured redshift, while the small dots are the 3σ radio upper limits with no spectroscopic z. The dashed line is the best-fitting relation obtained considering only the radio detections with spectroscopic redshift, while the dot-dashed line is the best-fitting relation obtained by also taking into account the radio upper limits (and objects without spectroscopic redshift) through the ASURV package (Isobe et al. 1986). Right-hand panel – radio-to-MIR luminosity ratio versus MIR luminosity. Symbols, as well as the dashed and dot-dashed lines, are the same as in the left-hand panel. The dotted line is the local radio–FIR correlation converted into radio–MIR through the empirical relations between $L_{\rm FIR}$ and $L_{15\,\mu\rm m}$ found locally by Elbaz et al. (2002). The triple-dot-dashed line is the best-fitting relation found by Garrett (2002) for a radio–MIR sample in the HDF-N.

with a dispersion of ~0.27 dex. Slope, normalization and dispersion are consistent, within errors, with those of the local determination of the radio–FIR relation found for *IRAS* galaxies by Yun et al. [2001; $\log(L_{1.4\,\rm GHz}) \propto (0.99 \pm 0.01)\log(L_{60\,\mu\rm m})$; $\sigma = 0.26$]. Because our determination does not take into account the radio upper limits (about 3/4 of the total), it is more representative of the upper envelope (i.e. the brighter radio objects) than of the 'real' radio–MIR luminosity distribution. In order to include the MIR galaxies not detected in the radio, we have recomputed the radio–MIR luminosity correlation for the entire sample of 331 MIR-selected galaxies by using ASURV (the Survival Analysis Package which uses the routines described in Isobe, Feigelson & Nelson 1986 and takes into account also the upper or lower limits in a sample). A redshift has been assigned to the 192 sources without spectroscopic information by using the empirical correlation (and its spread) between the 15-μm flux densities and redshifts found for our 139 spectroscopically identified galaxies:

$$\log(z) = -(0.68 \pm 0.04) - (0.37 \pm 0.06)\log(S_{15\,\mu\rm m}[\rm mJy]) + G(0, \sigma_{\rm rel}) \quad (2)$$

where $\sigma_{\rm rel}$ (= 0.25) is the 1σ dispersion of the relation and $G(0, \sigma_{\rm rel})$ is a Gaussian distribution with centre 0 and width $\sigma_{\rm rel}$. For the extragalactic sources not detected in the radio we have adopted an upper limit to the 1.4-GHz flux density equal to their corresponding 3σ value on radio maps. Under these assumptions, we have re-determined the radio–MIR correlation through ASURV, obtaining:

$$\log(L_{1.4\,\rm GHz}/{\rm L}_\odot) = (1.08 \pm 0.04)\log(L_{15\,\mu\rm m}/{\rm L}_\odot) - (6.07 \pm 0.41) \quad (3)$$

with a dispersion of ~0.34 dex. This relation, shown as dot-dashed line in the left-hand panel of Fig. 1, is somewhat more scattered than and lies about a factor of 2 below the previous determination. The right-hand panel of Fig. 1 shows the radio-to-MIR luminosity ratio versus MIR luminosity. Our estimate of the 'real' correlation (dot-dashed line) has a lower normalization than the local radio–FIR correlation (dotted line; extrapolated to radio–MIR as described below), which is instead much closer to our determination for detections only (dashed line). The local relation corresponds to a local value of the 'q' parameter equal to 2.34 [defined as $q \equiv \log[L_{\rm FIR}[W]/(3.75 \times 10^{12}[\rm Hz]) \times 1/L_{1.4\,\rm GHz}[W\,\rm Hz^{-1}]]$, where the FIR flux is defined to be $1.26 \times 10^{-14}(2.58\ S_{60\,\mu\rm m} + S_{100\,\mu\rm m})$ [W m^{-2}]; see Condon, Anderson & Helou 1991] and is converted to MIR through the empirical relations between $L_{\rm FIR}$ and $L_{15\,\mu\rm m}$ found for local galaxies by Elbaz et al. (2002). In the same figure we also show the relation derived (using the same K-corrections and cosmological parameters considered in our analysis) from the radio and 15-μm data for 19 *ISOCAM* sources detected in the WSRT deep radio survey of the *Hubble Deep Field*-north (HDF-N) region (see table 1 in Garrett 2002). This radio–MIR correlation (shown as dot-dot-dot-dashed line in the figure) has a normalization significantly higher (about a factor of 5) than our best-fitting relation and is also higher than the local one. Note, however, that this relation is derived using only the radio detections with spectroscopic z, without taking into account the radio upper limits. Because the number of upper limits is similar to that of the detections (which constitute ~40 per cent of the 15-μm sample detected at $>5\sigma$ level), it is likely that, as we find for our data, the 'real' correlation would have a somewhat lower normalization. Despite this, the comparison of our data with those in the HDF-N region suggests a possible change in normalization of the radio–MIR correlation at the higher redshifts sampled by the HDF-N *ISO* selected galaxies. Alternatively, the two sets of data (ELAIS and HDF-N surveys) could be made consistent with each other if the *ISO* or the radio data in the two fields were on a different flux scale (i.e. underestimated *ISO* or overestimated radio flux densities in the HDF-N).

Despite the difference in normalization between our radio–infrared correlation and the local one, which seems to suggest a change in the radio–infrared correlation with redshift, the important result of our analysis is that radio and MIR luminosities for galaxies strongly correlate with each other, almost as well as that found for the radio and FIR, and at significantly higher redshifts than those explored by *IRAS*. This implies a possible correlation between the PAH emission and the radio (and FIR) luminosity. The somewhat larger dispersion with respect to that observed for the radio–FIR relation is due either to the large spread in the mixture of PAH and thermal emission at the high temperatures responsible for the radiation observed in the MIR band, or to the complicated shape of the galaxy SEDs in that waveband, which introduces uncertainties and significant object-to-object variations in the MIR *K*-correction.

Fig. 2 shows the ratio between 1.4-GHz and 15-μm flux densities as a function of redshift for our spectroscopically identified sample of galaxies with radio detections. The dashed line shows the expected change of this ratio due to the different *K*-corrections (for starburst galaxies) in the two bands. The normalization of this curve has been chosen so that approximately the same number of objects lie above and below the line. This corresponds to a value $\langle S_{1.4\,\mathrm{GHz}}/S_{15\,\mu\mathrm{m}}\rangle \simeq 0.15$ at $z = 0$. This value is in good agreement with the value obtained by combining the well known 1.4-GHz/60-μm relation – $S_{60\,\mu\mathrm{m}} \simeq 127 S_{1.4\,\mathrm{GHz}}$ (Cram et al. 1998) – and the average 15-/60-μm ratio found by Mazzei et al. (2001) and Xu (2000) – $\langle S_{15\,\mu\mathrm{m}}/S_{60\,\mu\mathrm{m}}\rangle \simeq 0.05$ (note, however, above that our radio detections describe the upper envelope – i.e. stronger radio sources – of the radio–MIR correlation, rather than the entire population). Despite the relatively large spread in the values of the radio–MIR flux density ratio, no obvious trend with redshift is seen in our data for $z \gtrsim 0.07$. All the objects below this redshift show values of their radio to MIR flux density ratios which are significantly lower than the mean. One possible reason for this might be that we have missed some extended emission in some of these sources. In fact, about half of the very low redshift sources have a weak radio emission (detected below the 5σ threshold) therefore, because of the low signal-to-noise ratio, their flux density may have been underestimated if their radio emission is more extended than the beam (∼15 arcsec). Indeed, most of these faint radio sources at low redshift are bright and extended in both optical and MIR (∼40 arcsec to 1 arcmin).

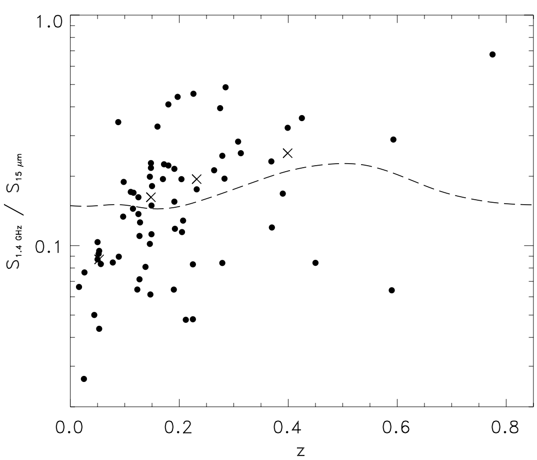

Figure 2. Radio/MIR flux density ratios versus redshift for our spectroscopically identified galaxies. Diagonal crosses are the median values of the ratio in different redshift intervals ($z < 0.1$, $0.1 \leqslant z < 0.2$, $0.2 \leqslant z < 0.3$ and $z \geqslant 0.3$), plotted in correspondence of the median redshift. The dashed line shows the expected change with z of $S_{1.4\,\mathrm{GHz}}/S_{15\,\mu\mathrm{m}}$ due to the difference between the average radio and MIR starburst *K*-corrections (normalized to the median value for our data, corresponding to $S_{1.4\,\mathrm{GHz}}/S_{15\,\mu\mathrm{m}} = 0.15$) at $z = 0$.

4 CONTRIBUTION OF MIR GALAXIES TO THE RADIO SOURCE COUNTS

In order to estimate the contribution made to the radio source counts from infrared galaxies, we have convolved the correlation between radio and 15-μm luminosities derived in the previous section with the evolutionary model for spiral and starburst galaxies which fits the 15-μm source counts in S1 (Gruppioni et al. 2002). The intrinsic dispersion adopted for the radio–MIR correlation ($\sigma \sim 0.28$ dex) has been derived by subtracting from the observed value (∼0.34 dex) the estimated contributions from the uncertainties on the radio and 15-μm observed flux densities (∼0.08 and 0.10 dex, respectively) and the radio and 15-μm *K*-corrections (∼0.02 and 0.15 dex, respectively). The resulting predicted source counts for starburst + Seyfert 2, normal spiral and all galaxies are plotted in Fig. 3 as dashed, dotted and solid lines, respectively. As a consistency check, we have derived the radio counts of our *ISO*-selected galaxies directly from the data. Each radio-detected *ISO* galaxy has been weighted by its radio and MIR spatial coverage and the contribution from all the radio detections in radio bins have been summed to produce the counts shown as filled circles in Fig. 3. The data points are in excellent agreement with the model predictions; in particular, the star-forming population would be responsible for about 40–60 per cent of the observed counts at $S_{1.4\,\mathrm{GHz}} \sim 50$–100 μJy. Therefore, starburst galaxies would make up most of the observed radio counts at μJy levels, in agreement with the results from very deep radio surveys, such as that in the HDF-N, where ∼80 per cent of sources detected at $S_{1.4\,\mathrm{GHz}} > 16$ μJy have been identified with starburst galaxies (Richards 2000). Conversely, the fractional contribution of starburst galaxies to the radio counts decreases rapidly above $S_{1.4\,\mathrm{GHz}} \sim 0.1$ mJy; this is in good agreement with spectroscopic identifications at the sub-mJy level, which find ∼60–70 per cent of elliptical galaxies and AGN1 among the optical counterparts of $S_{1.4\,\mathrm{GHz}} \gtrsim 0.2$ mJy radio sources (Gruppioni et al. 1999).

Given the differences in the normalization of the relations between radio and MIR luminosities derived from different samples (see previous section), we have computed the expected radio counts by increasing the normalization of our best-fitting correlation by a factor of 2, in such a way to bring it to the same scale as the local correlation. The resulting (total) counts are shown by the thin solid line in Fig. 3. The higher normalization relation produces a contribution to the radio counts which is far too high with respect to the observed data and exceeds the total radio counts at $S_{1.4\,\mathrm{GHz}} \lesssim 0.3$ mJy. Of course, this result is produced by the combination of the radio–MIR correlation and a model fitting the source counts. However, the model considered here is the only one able to fit the 15-μm counts in S1, which are lower than the other existing ones. Therefore, a radio–MIR correlation with a normalization significantly higher than that found in this work seems to be inconsistent with the observed faint 1.4-GHz source counts.

5 CONCLUSIONS

By searching for 3σ detections on deep ATCA 1.4-GHz maps of the southern ELAIS fields S1 and S2, and cross-correlating these with

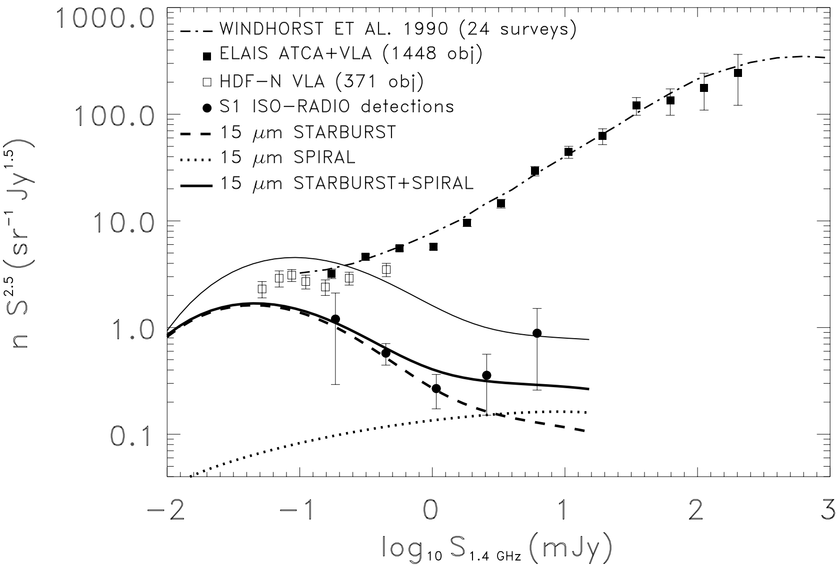

Figure 3. Best-fitting model to our ELAIS 15-μm extragalactic source counts (in differential form, normalized to a Euclidean non-evolving distribution) converted to 1.4 GHz by considering the empirical relation found for our data and its spread. As explained in the plot, the thick solid line represents the expected total source counts, while the short-dashed and the dotted lines are respectively the modelled contributions of a population of strongly evolving starburst galaxies (plus Seyfert 2) and non-evolving spirals. The thin solid line is the total contribution from starburst and spiral galaxies obtained by increasing the radio–MIR relation normalization by a factor of 2. The filled circles are the counts of the S1 15-μm sources with a $\geqslant 3\sigma$ 1.4-GHz counterpart. The dot-dashed line represents the fit of Windhorst, Mathis & Neuschaefer (1990) to the 1.4-GHz counts obtained from 24 different radio surveys. The filled squares are the total radio counts in the ELAIS regions (a combination of the S1 ATCA data of Gruppioni et al. 1999 with the VLA data in the northern ELAIS regions of Ciliegi et al. 1999). The open squares are the 1.4-GHz counts in the HDF-N from Richards (2000).

15-μm extragalactic objects detected, respectively, by Lari et al. (2001) and Pozzi et al. (2003), we have obtained a sample of 84 MIR–radio galaxies (65 of which have measured redshifts).

These data have allowed us for the first time to study with a statistically significant sample of objects the radio–MIR correlation and the radio and infrared properties of galaxies to much larger distances and fainter flux densities than previously achieved with *IRAS*.

The principal results of our analysis are as follows.

(i) The radio–MIR correlation for MIR-selected galaxies with a radio detection in our radio maps is well described by an approximately linear relation, with a scatter of $\sim$0.27 dex (similar to that found for the local radio–FIR relation), implying that PAH band emission correlates with FIR and radio luminosity and that the locally determined correlation between radio and infrared emission for star-forming galaxies persists to cosmological distances ($z \sim 0.6$).

(ii) If we consider also the radio upper limits we can obtain an estimate of the 'real' radio–MIR correlation, unbiased by the radio non-detections. We still obtain a strong correlation between radio and MIR luminosities, but with a normalization that is lower by a factor of 2 and a larger spread ($\sim$0.34 dex). The lower normalization of our relation corrected for upper limits with respect to the local radio–MIR relation (derived from the radio–FIR through a local FIR/MIR average ratio) implies a change in the radio–MIR correlation with increasing redshift.

(iii) There is no indication of any trend with z in the radio–MIR correlation found for our data (apart from the K-correction effects), up to $z \sim 0.6$.

(iv) The contribution of 15-μm galaxies to the radio source counts has been computed directly from our data and also by including the empirical radio–MIR correlation and its spread into the model that fits the MIR extragalactic source counts. Data and model agree very well and predict that MIR starburst galaxies should start contributing significantly ($\gtrsim$10 per cent) to the radio counts around 0.5–0.8 mJy, with their importance rapidly increasing until they make up >40–60 per cent of the observed counts at $S_{1.4} \lesssim$ 50–100 μJy.

ACKNOWLEDGMENTS

Part of this work was supported by MIUR (Cofin) and ASI research grants.

REFERENCES

Aussel H., Césarsky C. J., Elbaz D., Starck J.-L., 1999, A&A, 342, 313
Cesarsky C. J. et al., 1996, A&A, 315, L32
Ciliegi P. et al., 1999, MNRAS, 302, 222
Condon J. J., 1992, ARA&A, 30, 57
Condon J. J., Anderson M. L., Helou G., 1991, ApJ, 376, 95
Cram L., Hopkins A., Mobasher B., Rowan-Robinson M., 1998, ApJ, 507, 155
Elbaz D. et al., 1999, A&A, 351, L37
Elbaz D., Cesarsky C. J., Chanial D., Aussel H., Franceschini F., Fadda D., Chary R. R., 2002, A&A, 384, 848
Franceschini A., Aussel H., Cesarsky C. J., Elbaz D., Fadda D., 2001, A&A, 378, 1
Garrett M. A., 2002, A&A, 284, L19
Gruppioni C., Mignoli M., Zamorani G., 1999, MNRAS, 304, 199
Gruppioni C., Lari C., Pozzi F., Zamorani G., Franceschini A., Oliver S., Rowan-Robinson M., Serjeant S., 2002, MNRAS, 335, 831
Gruppioni C. et al., 1999, MNRAS, 305, 297
Isobe T., Feigelson E. D., Nelson P. I., 1986, ApJ, 306, 490
Kessler M. F. et al., 1996, A&A, 315, 27
Lari C. et al., 2001, MNRAS, 325, 1173

Mazzei P., Aussel H., Xu C., Salvo M., De Zotti G., Franceschini A., 2001, New Astron., 6, 265
Oliver S. et al., 2000, MNRAS, 316, 749
Pozzi F. et al., 2003, MNRAS, in press
Puget J.-L., Léger A., ARA&A, 1989, 27, 161
Richards E. A., 2000, ApJ, 533, 611
Windhorst R. A., Mathis D. F., Neuschaefer L. W., 1990, in Kron R. G., ed., ASP Conf. Ser. Vol. 10, Evolution of the Universe of Galaxies. Astron. Soc. Pac., San Francisco, p. 389
Xu C., 2000, ApJ, 541, 134
Yun M. S., Reddy N. A., Condon J. J., 2001, ApJ, 554, 803

This paper has been typeset from a TEX/LATEX file prepared by the author.